Available online at www.sciencedirect.com
ScienceDirect
Energy Procedia 36 (2013) 268 – 277
Energy Procedia

TerraGreen 13 International Conference 2013 - Advancements in Renewable Energy and Clean Environment

Slug Flow-Heat Transfer in Parallel Plate Microchannel Including Slip Effects and Axial Conduction

Mourad Mecili[a]*, El Hacene Mezaache[b]

[b]*Laboratoire de Recherche sur la Physico-chimie des Surfaces et Interfaces, Université de Skikda, BP 26, Skikda 21000, Algérie*
[b] *Département des Sciences de la Matière, Faculté des Sciences, Université de Skikda, BP 26, Skikda 21000, Algérie*

Abstract

In this paper the forced convection with slug flow model in parallel plate microchannel is studied. In the slug flow model, it is assumed that the velocity of the fluid is uniform across any cross-section perpendicular to the axis of the microchannel. The microscale analysis is taking into account by including the jump temperature at the surface. The axial conduction within the fluid is included but the viscous dissipation is neglected. The energy equation is solved by finite integral transform technique. The isoflux and isothermal boundary conditions were applied. The local and fully developed Nusselt numbers have been obtained in terms of the Knudsen number and Peclet number.

Keywords: forced convection; slug flow; parallel plate microchannel; jump temperature; integral transform technique.

1. Introduction

Convection heat transfer in micro-conduits is encountered in many industrial processes such as biomedical diagnostic technique, biochemical application, microelectromechanical systems (MEMS), cryogenics, thermal control of electronic devices, chemical separation processes, aerospace engineering, vacuum technology, accelerometer flow sensors, micro nozzles, micro valves.

The researchers classified the gas flow in microchannel into four flow regimes: continuum flow regime (Kn<0.001), slip flow regime (0.001<Kn≤0.1), transition flow regime (0.1<Kn≤10) and free molecular flow regime (Kn>10). Knudsen number Kn characterises the rarefaction effect and it is defined as the ratio of the molecular mean free path to the characteristic length of the microchannel. In the slip flow regime,

* Corresponding author. Tel.: +0-213-38-701012; fax: +0-213-38-701012
E-mail address: mmourad_75@yahoo.fr.

doi:10.1016/j.egypro.2013.07.031

the flow and the heat transfer phenomena are described by the continuum governing equations subjected to the slip conditions at the wall [1]. As a results of slip at the surface, the fluid particle have a tangential velocity at the wall called slip velocity, and a finite temperature difference at the surface called the temperature jump. The gas-surface interactions are characterized by two parameters, namely F_m and F_t, where: F_m is the tangential momentum accommodation factor which represents the fraction of the molecules undergoing diffuse reflection, F_m=1 for heavy atoms and F_m≠1 for light atoms [2], and F_t is the thermal accommodation factor.

The slip flow-heat transfer of incompressible gaseous flowing in microtubes was reviewed by [1–7]. [1] studied the convective heat transfer subjected to isothermal boundary condition without viscous dissipation, and discussed the rarefaction effect trough the recalling factor. The energy equation was solved by separation of variables method based on hypergeometric expansion eigenfuction, The eigenvalues were computed by a new asymptotic approach. It is found that the heat transfer depends both on the degree of rarefaction and on the surface accommodation coefficients. The authors indicate that the rarefaction increases the heat transfer when the jump temperature is neglected or insignificant, for large jump temperature at wall the rarefaction diminishes the heat transfer. [2] examined the microflow heat transfer for laminar rarefied gas flow including viscous dissipation subjected to constant wall temperature, constant wall heat flux and linear variation wall temperature boundary conditions. The energy equation was solved by the finite volume method. The effects of Brinkman and Knudsen numbers on Nusselt number were observed for thermal entrance and fully developed regions. [3] analyzed the convective heat transfer for steady state, laminar fully developed flow taking into account the viscous dissipation, slip velocity and jump temperature. The energy equation was solved by integral transform technique for isothermal and isoflux conditions. The effects of Knudsen, Brinkman and Prandlt numbers on heat transfer were illustrated. The authors observed that the slip velocity and temperature jump have opposite effects on the Nusselt number. [4] investigated the extended Graetz problem by considering the rarefaction effect, viscous dissipation and axial heat conduction under uniform wall temperature boundary condition. The energy equation was solved numerically and the solution domain was extended to infinite. The effect of Peclet number on local Nusselt number was discussed. The authors showed that the fully developed Nusselt number and the thermal entrance length increase with the decreasing Peclet number. [5] studied the microscale heat transfer with constant wall heat flux thermal boundary condition. The rarefaction, the viscous dissipation and the axial conduction were included. The energy equation was solved analytically by using general eigenfunction expansion. The authors have found that the local Nusselt number decreases with increasing Knudsen and Brinkman numbers. The local Nusselt numbers converges to the same fully-developed value for all values of Peclet and Brinkman numbers. The thermal entrance length increases with decreasing Peclet number. [6] analysed the hydrodynamically and thermally fully developed flow by including viscous dissipation. Isothermal and isoflux thermal boundary conditions have been considered. [7] examined the convective heat transfer in an infinite microtube subjected to mixed boundary conditions, taking into account the axial conduction and the rarefaction. The velocity was considered to be constant (slug flow). The energy equation has been solved by variables separation method. The authors observed that the local Nusselt number increases with increase in Peclet number but decreases with increase in Knudsen number. The fully-developed Nusselt number decreases with increase in Knudsen number but, for a fixed value of Knudsen number, it reaches to a constant value for all Peclet number values.

Slip flow–heat transfer of incompressible gaseous in parallel plate microchannel was conducted by [8–10].

[8] studied the effect of shear work at solid boundaries in small scale gaseous flows where slip effects were included. The author illustrated the effect of shear work at the boundary on convective heat transfer subjected to the constant wall heat flux boundary condition in the slip-flow regime.

Nomenclature

b	defined in (eq. 47)		X	dimensionless horizontal coordinate	
F_T	thermal accommodation coefficient		y	vertical coordinate	m
h	convective heat transfer coefficient	W $m^{-2}K^{-1}$	Y	dimensionless vertical coordinate	
k	thermal conductivity	W m^{-1} K^{-1}	***Greek symbols***		
Kn	Knudsen number		α	thermal diffusivity	m^2s^{-1}
L	half distance between plates	m	γ	specific heat ratio	
Nu	Nusselt number		λ	molecular mean free path	m
Pr	Prandlt number		θ	dimensionless temperature	
Pe	Peclet number		***Subscripts***		
q_w	wall heat flux	W m^{-2}	b	bulk	
T	Temperature	K	s	fluid properties at the wall	
u	Velocity	m s^{-1}	w	wall	
x	horizontal coordinate	m	∞	fully developed	

[9] studied the extended Graetz problem including viscous dissipation and axial heat conduction. The energy equation for both isothermal and isoflux conditions was solved by using eigenfunctions expansion. The effects of Peclet number, Knudsen number, Brinkman number on heat transfer were showed. The results indicate that the Nusselt number decreases as Knudsen number or Brinkman number increases and as Peclet number decreases.

The microscale heat transfer for slip flow regime in rectangular microchannal was analysed by [11–13].

[11] used the integral transform technique to derive the velocity and the temperature distributions under constant wall temperature boundary condition subjected to the eight possible thermal versions. It is found that with the perfect accommodation for velocity and temperature, the rarefaction effect decreases the heat transfer for the eight thermal versions. [12] numerically solved the Navier-Stokes and energy equations by control-volume method. The effects of Reynolds number, channel aspect ratio and Knudsen number on the simultaneously developing velocity, temperature fields, entrance length, friction coefficient and Nusselt number are examined in detail. The authors have shown that in the entrance region very large reductions were observed in the friction factor and Nusselt number due to rarefaction effects.

[13] determined the temperature profile by using the mathematical similarity between the heat conduction and convection under constant wall heat flux boundary condition. Additionally the average Nusselt number was determined for any all eight thermal versions. The authors showed that the rarefaction decreases the heat transfer.

Recently, [14] reviewed the problem of forced convective heat transfer in microtube and parallel plate microchannel for slip flow regime in presence of the viscous dissipation under isothermal boundary condition. The authors concluded that the heat transfer depends on both degree of rarefaction, measured by $Kn\beta_v$ (or slips radius p), and jump temperature magnitude measured by β parameter. The slip velocity and the jump temperature have opposite effects on heat transfer.

2. Analysis and results

In this study, the conventional slug flow (constant velocity) problem in a parallel plate microchannel is extended to include the microscale characteristics as well as the axial conduction effect. The analysis is

based on steady, laminar, slug flow of an incompressible rarefied gaseous in a parallel plate microchannel. The first order jump temperature at the surface is incorporated.

2.1. Constant wall temperature

The energy equation under the previous assumptions can be written as:

$$u_0 \frac{\partial T}{\partial x} = \alpha \left[\frac{\partial^2 T}{\partial y^2} + \frac{\partial^2 T}{\partial x^2} \right] \tag{1}$$

Where T is the temperature, u_0 the uniform velocity, x the longitudinal coordinate, y is the transversal coordinate and α is the thermal diffusivity.

The boundary conditions are follows as:

$$T(x=0,y) = T_0 : 0 \le y \le L \tag{2}$$

$$T(y=L) = T_s = T_w - \frac{2-F_T}{F_T} \frac{2\gamma}{\gamma+1} \frac{\lambda}{\mathrm{Pr}} \left(\frac{\partial T}{\partial y} \right)_{y=L} \qquad \left(\frac{\partial T}{\partial y} \right)_{y=0} = 0 \tag{3, 4}$$

Where L is the half distance between plates, λ the molecular mean free path, T_s the temperature of the gas at the wall, T_w the wall temperature, F_T the thermal accommodation coefficient, Pr the Prandlt number and γ is the specific heat ratio.

Now, we introduce the non-dimensional quantities as follows:

$$\theta = \frac{T - T_s}{T_0 - T_s} \qquad Y = \frac{y}{L} \qquad X = \frac{x}{L\,Pe} \qquad Pe = \frac{u_0 L}{\alpha} \tag{5}$$

The dimensionless energy equation and dimensionless boundary conditions are given by:

$$\frac{\partial \theta}{\partial X} = \frac{\partial^2 \theta}{\partial Y^2} + \frac{1}{Pe^2} \frac{\partial^2 \theta}{\partial X^2} \qquad \theta(X=0,Y) = 1 \qquad \theta(X,Y=1) = 0 \qquad \left[\frac{\partial \theta}{\partial Y} \right]_{Y=0} = 0 \tag{6-9}$$

2.1.1. Integral transform technique solution

To solve the energy equation eq. (1) with the boundary conditions eqs. (2-4), we use the integral transform technique based on eigenfunctions and eigenvalues [15].

The eigenfunctions-eigenvalues problem can be represented by the following ordinary differential equation:

$$\frac{d^2 \Phi_i(Y)}{dY^2} + \varepsilon_i^2 \Phi_i(Y) = 0 \tag{10}$$

Where $\Phi_i(Y)$ are the eigenfunctions, and ε_i are the eigenvalues. The eigenfunctions $\Phi_i(Y)$ are subject to the following boundary conditions:

$$\Phi_i(Y=1)=0 \quad \left(\frac{d\Phi_i}{dY}\right)_{Y=0}=0 \tag{11, 12}$$

The solution of the ordinary differential equation eq. (10) under the boundary condition eq. (12), gives the eigenfunctions expression

$$\Phi_i(Y)=\cos(\varepsilon_i Y) \tag{13}$$

The application of boundary condition eq. (11), gives the following transcendental equation:

$$\cos(\varepsilon_i)=0 \tag{14}$$

Using the above equation, the eigenvalues ε_i are directly expressed as follows

$$\varepsilon_i=(2i-1)\frac{\pi}{2} : i=1,2,.....n \tag{15}$$

Now, we introduce the integral transform of temperature and the inverse transform as follows:

$$\theta_i^*(X)=\int_0^1 \Phi_i(Y)\theta(X,Y)dY \qquad \theta(X,Y)=\sum_{i=1}^{\infty}\left(\frac{1}{N_i}\right)\Phi_i(Y)\theta_i^*(X) \tag{16, 17}$$

The factor N_i is obtained by application of the normalization condition:

$$\int_0^1 \Phi(\varepsilon_i,Y)\Phi(\varepsilon_j,Y)=\begin{cases}0 : i\neq j\\ N(\varepsilon_i) : i=j\end{cases} \qquad N_i=\int_0^1 \Phi_i^2(Y)dY \tag{18, 19}$$

Multiplying the both sides of eq. (6) by (Φ), and integrated over the domain $0\leq Y\leq 1$, the dimensionless energy equation becomes:

$$\frac{1}{Pe^2}\frac{d^2\theta_i^*(X)}{dX^2}-\frac{d\theta_i^*(X)}{dX}-\varepsilon_i^2\theta_i^*(X)=0 \tag{20}$$

With the boundary condition:

$$\theta_i^*(X=0)=\int_0^1 \Phi_i(Y)dY \tag{21}$$

The solution of the second order ODE problem, eq. (20), subject to the boundary condition, eq. (21), is obtained as:

$$\theta_i^*(X)=Q_i\exp\left[\frac{XPe^2(1-M_i)}{2}\right] \tag{22}$$

Where:

$$Q_i = \int_0^1 \Phi_i(Y)dY \qquad M_i = \sqrt{1+4\varepsilon_i^2/Pe^2} \tag{23}$$

The substitution of eq. (22) into eq. (17), gives the dimensionless temperature profile

$$\theta(X,Y) = \sum_{i=1}^{\infty} \frac{Q_i \Phi_i(Y)}{N_i} exp\left[\frac{X.Pe^2(1-M_i)}{2}\right] \tag{24}$$

2.1.2. Determination of local Nusselt number

Based on heat convection coefficient *h*, the local Nusselt number is given by

$$Nu(X) = \frac{h(4L)}{k} = \frac{-4[\partial\theta/\partial Y]_{Y=1}}{\theta_b(X) - 2bKn[\partial\theta/\partial Y]_{Y=1}} \tag{25}$$

Where

$$\theta_b(X) = \int_0^1 \theta(X,Y)dY \quad Kn = \frac{\lambda}{2L} \tag{26}$$

2.2. Constant wall heat flux

The dimensionless energy equation and boundary conditions are given by:

$$\frac{\partial\theta}{\partial X} = \frac{\partial^2\theta}{\partial Y^2} + \frac{1}{Pe^2}\frac{\partial^2\theta}{\partial X^2} \qquad \theta(X=0,Y)=0 \qquad \left[\frac{\partial\theta}{\partial Y}\right]_{Y=0} = 0 \qquad \left[\frac{\partial\theta}{\partial Y}\right]_{Y=1} = 1 \tag{27-30}$$

In this case (constant wall heat flux), the dimensionless temperature is defined as

$$\theta = (T - T_0)/(q_w L/k) \tag{31}$$

2.2.1. Determination of fully developed temperature profile

The fully developed temperature profile can be expressed by the superposition form

$$\theta_\infty(X,Y) = A\,X + g(Y) \tag{32}$$

Where *A* is constant that needs to be determined. Substituting eq. (32) into eq. (27), and integrating in *Y* direction results in:

$$g(Y) = \frac{A\,Y^2}{2} + B\,Y + C \tag{33}$$

Using the boundary condition at the microchannel center, eq. (29), constant *B* can be determined as zero. Using the boundary condition at the wall, eq. (30), we obtain *A*=1. Thus:

$$g(Y)=\frac{Y^2}{2}+C \qquad \theta_\infty(X,Y)=X+\frac{Y^2}{2}+C \tag{34, 35}$$

Integrating eq. (27) in X direction, we obtain

$$\theta=\int_0^X \frac{\partial^2\theta}{\partial Y^2}dX+\frac{1}{Pe^2}\frac{\partial\theta}{\partial X} \tag{36}$$

Integrating eq. (36) in Y direction from 0 to 1 and taking into account the boundary conditions eq. (29) and eq. (30)

$$\int_0^1 \theta dY = X+\frac{1}{Pe^2}\frac{\partial}{\partial X}\left(\int_0^1 \theta dY\right) \tag{37}$$

$$\int_0^1 (X+\frac{Y^2}{2}+C)dY = X+\frac{1}{Pe^2}\frac{\partial}{\partial X}\left(\int_0^1 (X+(Y^2/2)+C)dY\right) \tag{38}$$

After the integration, we obtain the constant C:

$$C=1/Pe^2-1/6 \tag{39}$$

Fully-developed temperature can be obtained by substituting eq. (39) into eq. (35) as

$$\theta(X,Y)=X+\frac{Y^2}{2}+\frac{1}{Pe^2}-\frac{1}{6} \tag{40}$$

2.2.2. Determination of fully developed Nusselt number

Introducing dimensionless quantities, fully-developed Nusselt number can be written as:

$$Nu_\infty=\frac{h_\infty(4L)}{k}=\frac{4}{\theta_{w\infty}-\theta_{b\infty}} \tag{41}$$

Where $\theta_{b\infty}$ is the fully developed dimensionless bulk temperature which is defined as:

$$\theta_{b\infty}(X)=\int_0^1 \theta_\infty(X,Y)dY \tag{42}$$

Substituting eq. (40) into eq. (42)

$$\theta_{b\infty}(X)=X+\frac{1}{Pe^2} \tag{43}$$

$\theta_{w\infty}$ is the fully developed wall temperature and can be determined by the implementation of the temperature jump in dimensionless form

$$\theta_{w\infty}=\theta_{s\infty}+2bKn \tag{44}$$

Where $\theta_{s\infty}$ is the fully developed gas temperature at the surface, it is defined as:

$$\theta_{s\infty} = \theta_{\infty}(Y=1,X) = X + \frac{1}{Pe^2} + \frac{1}{3} \tag{45}$$

Substituting eqs. (43), (44) and (45) into eq. (41), Nu_{∞} can be determined as:

$$Nu_{\infty} = \frac{12}{1+6bKn} \tag{46}$$

With:

$$b = \frac{2-F_T}{F_T}\frac{2\gamma}{\gamma+1}\frac{1}{Pr} \tag{47}$$

All calculations are carried out with specific heat ratio γ=1.4, Prandtl number Pr=0.7 and thermal accommodation coefficient F_T = 1. The values of Knudsen number Kn is varied between 0.001 and 0.1, which are the applicability limits of the slip-flow regime, and Peclet number Pe is varied between 1 and 100. The present solution is also reduced to that of a macroscale case, by setting Kn=0.

Table 1a reported the values of fully developed Nusselt number computed at different Knudsen number values, for isothermal condition, these values (Nu_{∞}) are evaluated from the following equation.

$$Nu_{\infty} = \frac{4\varepsilon_1 \, sin(\varepsilon_1)}{\int_0^1 cos(\varepsilon_1 Y)dY + 2b\,Kn\,\varepsilon_1\,sin(\varepsilon_1)} \tag{48}$$

Table 1a indicates that fully developed Nu jumps from 9.8696 (for Kn=0, no-slip flow) to 5.41552 (for Kn=0.1, limiting slip flow), indicating 82.25 % decrease.

Table 1b reported the values of fully developed Nusselt number computed at different Knudsen number values, for isoflux condition, these values (Nu_{∞}) are evaluated from eq. (46). Table 1b indicates that fully developed Nu jumps from 12 (for Kn=0, no-slip flow) to 6 (for Kn=0.1, limiting slip flow), indicating 100 % decrease.

Table 1. Variation of fully developed Nusselt number with Knudsen number

Kn	Nu_{∞} *(a: isothermal condition)*	Nu_{∞} *(b: isoflux condition)*
0.0	9.8696	12
0.02	8.47545	10
0.04	7.42641	8.57143
0.06	6.60846	7.5
0.08	5.95281	6.66667
0.1	5.41552	6.0

In Fig. 1a, the effect of Pe number on local Nusselt number is demonstrated without the rarefaction effect (Kn=0). The data from this figure reveal that when the axial heat conduction within the fluid is included, the conductive heat transfer is assisting to the convective heat transfer, and this assistance is more significant by decreasing Pe number. Fig. 1a indicates also that the local Nusselt numbers (computed for different Pe numbers) take higher values near the microconduit entrance and monotonically decrease longitudinally along the microconduit. It may also be observed that the local Nusselt number and the thermal entrance length increase with decrease in Pe. In the thermally fully

developed region the all Nusselt numbers computed for different *Pe* numbers converge to the same asymptotic value. In other words the fully developed Nusselt number does not depends on Peclet number, the same results was reported by [7]. Fig. 1b illustrates the effect of rarefaction represented by *Kn* on local Nusselt number, and with *Pe* =10. It can be realized that Nusselt numbers are infinite at the entrance (at $X = 0$) and decays to their asymptotic (fully-developed) values.

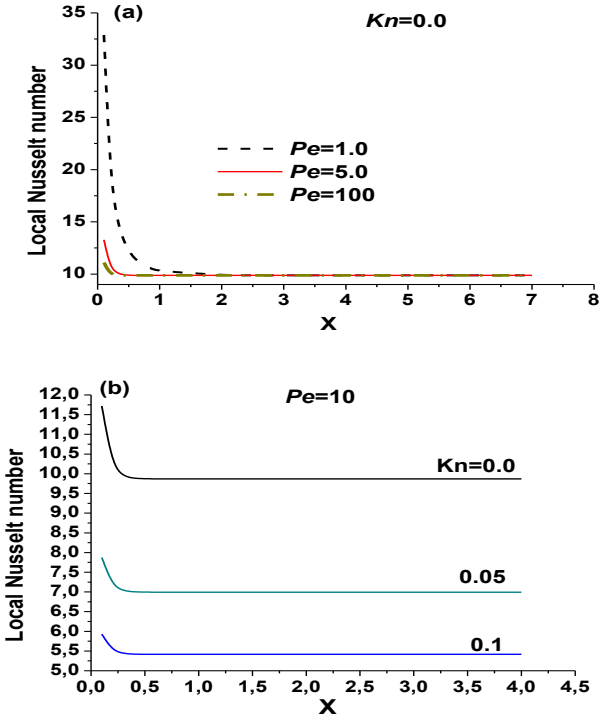

Fig. 1. Axial variation of local Nusselt number for isothermal conditions with *Kn*=0.0 (a), and *with Pe*=10 (b).

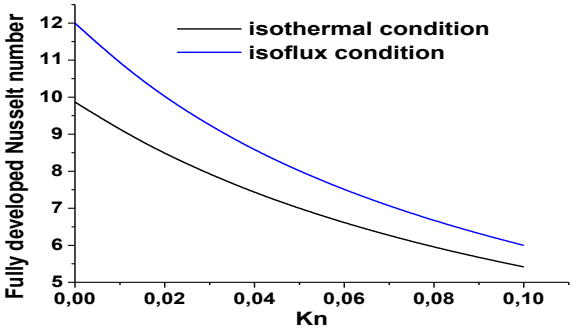

Fig. 2. Variation of fully developed Nusselt number with Kn, for isothermal and isoflux boundary conditions.

It is seen that Nusselt number always decreases with increase in *Kn* and this trend is in agreement with results reported in [2,3,7,9], this result may be explained by noting that, as the flow departs from the continuum behavior, a reduction in heat transfer at the surface occurs because the temperature gradient at the surface becomes smaller due to the temperature jump. Therefore, as *Kn* increases, the temperature jump increases and leads to decrease in the temperature gradient at the wall, consequently, the heat transfer decreases.

3. Conclusion

In this study, the conventional slug flow problem in parallel plate microchannel was extended to include both slip-flow characteristics and axial conduction effect. The energy equation is solved analytically by the infinite integral transform technique and, closed form solutions for temperature profile, bulk temperature and Nusselt number are derived in terms of Peclet number and Knudsen number. It is concluded that: (i) In the thermal entrance region, the local Nusselt number increases as Peclet number decreases but decreases as Knudsen number increases. (ii) The thermal entrance length increases as Peclet number decreases. (iii)The fully-developed Nusselt number decreases with increase in Knudsen number but, for a fixed value of Knudsen number, it reaches a constant value for all Peclet numbers.

References

[1] Larrodè FE, Housiadas C, Drossinos Y. Slip-flow heat transfer in circular tubes. *Int J Heat Mass Transfer* 2000; **43**: 2669–80.

[2] Sun W, Kakaç S, Yazicioglu AG. A numerical study of single-phase convective heat transfer in microtubes for slip flow. *Int J of Thermal Sciences* 2007; **46**: 1084–94.

[3] Tunc G, Bayazitoglu Y. Heat transfer in microtubes with viscous dissipation. *Int J Heat Mass Transfer* 2001; **44**: 2395–403.

[4] Çetin B, Yazicioglu AG, Kakaç S. Fluid flow in microtubes with axial conduction including rarefaction and viscous dissipation. *Int commun in Heat and Mass Transfer* 2008; **35**: 535–44.

[5] Çetin B, Yazicioglu AG, Kakaç S. Slip-flow heat transfer in microtubes with axial conduction and viscous dissipation–An extended Graetz problem. *Int J of Thermal Sciences* 2009; **48**: 1673–78.

[6] Aydin O, Avcı M. Heat and fluid flow characteristics of gases in micropipes. *Int J Heat Mass Transfer* 2006; **49**: 1723–30.

[7] Satapathy AK. Slip flow heat transfer in an infinite microtube with axial conduction. *Int J of Thermal Sciences* 2010; **49**: 153–60.

[8] Hadjiconstantinou NG, Dissipation in small scale gaseous flows, *J of Heat Transfer* 2003; **125**: 944–47.

[9] Joeng N, Joeng JT. Extended Graetz problem including streamwise conduction and viscous dissipation in microchannel. *Int J Heat Mass Transfer* 2006; **49**: 2151–57.

[10] Aydin O, Avcı M. Analysis of laminar heat transfer in micro-Poiseuille flow. *Int J Thermal Sciences* 2007; **46**: 30–7.

[11] Kuddusi L. Prediction of temperature distribution and Nusselt number in rectangular microchannels at wall slip condition for all versions of constant wall temperature. *Int J of Thermal Sciences* 2007; **46**: 998–1010.

[12] Renksizbulut M, Niazmand H, Tercan G. Slip-flow and heat transfer in rectangular microchannels with constant wall temperature. *Int J of Thermal Sciences* 2006; **45**: 870–81.

[13] Kuddusi L, Cetegen E. Prediction of temperature distribution and Nusselt number in rectangular microchannels at wall slip condition for all versions of constant heat flux. *Int J of Heat and Fluid Flow* 2007; **28**: 777–86.

[14] Mecili M, Mezaache E. Analytical prediction for slip flow-heat transfer in microtube and parallel plate microchannel including viscous dissipation. *International Journal of Heat &Technology* 2011; **29**: 79-86.

[15] Mecili M, Mezaache E, Zeghmati B. Solution of the Graetz-Brinkman problem by integral transform technique. *Journal of Scientific Research,* 2010; **1**: 246-249.